



저작자표시-비영리-변경금지 2.0 대한민국

이용자는 아래의 조건을 따르는 경우에 한하여 자유롭게

- 이 저작물을 복제, 배포, 전송, 전시, 공연 및 방송할 수 있습니다.

다음과 같은 조건을 따라야 합니다:



저작자표시. 귀하는 원저작자를 표시하여야 합니다.



비영리. 귀하는 이 저작물을 영리 목적으로 이용할 수 없습니다.



변경금지. 귀하는 이 저작물을 개작, 변형 또는 가공할 수 없습니다.

- 귀하는, 이 저작물의 재이용이나 배포의 경우, 이 저작물에 적용된 이용허락조건을 명확하게 나타내어야 합니다.
- 저작권자로부터 별도의 허가를 받으면 이러한 조건들은 적용되지 않습니다.

저작권법에 따른 이용자의 권리는 위의 내용에 의하여 영향을 받지 않습니다.

이것은 [이용허락규약\(Legal Code\)](#)을 이해하기 쉽게 요약한 것입니다.

[Disclaimer](#)

Master's Thesis of Philosophy degree

**Periostin deficiency attenuates kidney
fibrosis in diabetic nephropathy via
improving pancreatic β -cell
dysfunction.**

POSTN 결여로 인한 췌장 β -세포 기능장애
개선에 따른 당뇨병 콩팥병 완화 효과

February 2023

**Graduate School of Medicine
Seoul National University
Translational Medicine Major**

Ara Cho

Periostin deficiency attenuates kidney fibrosis in diabetic nephropathy by improving pancreatic β -cell dysfunction.

지도 교수 이 정 표

이 논문을 의학석사 학위논문으로 제출함
2022년 10월

서울대학교 대학원
의학과 중개의학 전공
조 아 라

조아라의 의학석사 학위논문을 인준함
2023년 1월

위 원 장 김동기 (인)
부위원장 이정표 (인)
위 원 이민재 (인)

Abstract

Introduction: Diabetic nephropathy (DN), the most common cause of chronic kidney disease, is associated with kidney fibrosis. Previous study demonstrated that periostin (POSTN) plays an important role in kidney fibrosis. The purpose of this study was to investigate the role of POSTN in DN.

Method: POSTN and tenascin C (TNC) concentrations in urine samples from patients with DN were measured. Fifty milligrams/kilogram streptozotocin (STZ) was administered for 5 days after unilateral nephrectomy (UNXSTZ) to induce DN in both the wild-type and *Postn*-null mice. Four experimental groups were generated: wild-type sham (WT sham), wild-type UNXSTZ (WT STZ), *Postn*-null sham (KO sham), *Postn*-null UNXSTZ (KO STZ). After 20 weeks, the molecular expression of fibrosis markers and histological changes were evaluated. Blood glucose levels and urine albumin were periodically measured. As a cell model of DN, NRK 49F cells were cultured under TGF- β treatment. We stimulated INS-1 cells with streptozotocin and evaluated cell viability in these cells.

Results: The concentrations of POSTN and TNC increased according to the severity of DN in human samples. In contrast to the WT STZ model, the KO STZ model showed lower urine albumin excretion and less glomerular sclerosis and interstitial fibrosis. The KO STZ model had lower expression of fibrosis markers and TNC. The glucose level of the KO STZ model was well regulated in comparison with that of the WT STZ model. In addition, in the KO STZ model, pancreatic islet integrity and insulin expression were significantly more preserved. In *in vitro* models using NRK 49F cells, the degree of fibrosis was not significantly different between groups treated with TGF- β alone and TGF- β and recombinant POSTN (rPOSTN) together.

The anti-POSTN antibody treatment of INS-1 cells with streptozotocin resulted in a higher cell viability than treatment with streptozotocin alone.

Conclusion: The absence of POSTN in DN contributes to renal fibrosis alleviation by improving pancreatic β -cell function. Blocking POSTN could be a new treatment target for DN. Additionally, there is an association between POSTN and TNC.

Keywords: POSTN; DN; kidney fibrosis; TNC; β -cell dysfunction; UNXSTZ

Student Number: 2020-26768

Table of Contents

Abstract	iii
List of Figures	vi
List of Abbreviations	vii
Introduction	1
Materials and Methods	3
Results.....	11
Discussion	16
Figures	20
Reference	32
Abstract in Korean	36

List of Figures

Figure 1. A schematic overview of the animal model

Figure 2. Periostin and tenascin C levels measured in urine in patients with diabetic nephropathy

Figure 3. Functional data of the mouse groups

Figure 4. Analysis of data related to fibrosis among the groups of mice

Figure 5. The effect of periostin deficiency on the TGF- β 1/Smad pathway in a diabetic nephropathy model

Figure 6. TGF- β and periostin-induced fibrosis in NRK-49 cells

Figure 7. The role of periostin in pancreatic function

List of Abbreviations

Diabetic nephropathy (DN)

periostin (POSTN)

recombinant periostin (rPOSTN)

tenascin C (TNC)

streptozotocin (STZ)

Postn-null (periostin knock out B6 mice)

UNXSTZ model (Unilateral Nephrectomy – STZ injection)

Introduction

Diabetic nephropathy (DN) is the most common cause of chronic kidney disease (CKD) ¹, which is characterized by glomerulosclerosis and tubulointerstitial fibrosis, regardless of the cause. At present, there is no specific treatment method for DN other than controlling glucose levels and blood pressure well in advance of its onset.

Periostin (POSTN), a type of extracellular matrix protein, is found mainly in bones during growth. Its existence disappears after reaching adulthood ^{2,3}. After that, it can appear in a variety of tissues in disease states. For example, the expression of POSTN has been associated with a variety of pathological conditions, including asthma ⁴, heart failure ⁵, myocardial infarction ⁶, and metastases of various cancers ^{7,8,9}.

There has been emerging interest in the study of POSTN in the field of nephrology. Several studies have demonstrated that urinary POSTN levels are associated with tubular damage in renal fibrosis, as it is mainly expressed in tubulointerstitial areas ¹⁰. There is growing evidence that POSTN can be effectively used as a tissue or urinary biomarker for the diagnosis of type 2 diabetes ¹¹, lupus nephritis ¹², and IgA nephropathy ¹³.

There is a high level of POSTN expression in fibrotic tissues ^{14,15}. It has been found that POSTN is strongly correlated with the severity of CKD ¹⁶. Previous study reported that experimental inhibition of POSTN attenuates kidney fibrosis ¹⁷. Additionally, POSTN promotes kidney fibrosis through the p38 MAPK pathway after acute kidney injury triggered by hypoxia or ischemia–reperfusion injury ¹⁸. Recently, The expression of POSTN in the kidneys was found to increase with age, and the ablation of POSTN delayed aging ¹⁹.

However, there has been little research on the role of POSTN in DN. This study investigated the role of POSTN in the kidney and pancreas in DN models induced by streptozotocin (STZ).

Materials and Methods

Measurement of urine tenascin C (TNC) and POSTN levels in patients with DN

To evaluate an association between kidney function and urinary POSTN and/or TNC, the clinical data of 200 individuals with DN were collected, including age, sex, serum creatinine, estimated glomerular filtration rate (eGFR) and urine protein-to-creatinine ratio (UPCR). eGFR was calculated using the CKD-EPI creatinine equation. A POSTN ELISA kit (27751, IBL) and TNC ELISA kit (DY3548B, R&D system) were used to measure the urinary POSTN and TNC levels. All measurements were performed in a blinded manner in duplicate. Informed consent was obtained from the study participants before enrollment. The present study was conducted with the approval of the Research Ethics Committee of the Seoul National University Boramae Medical Center. All procedures were performed in accordance with the ethical standards of the institutional and/or national research committee and with the 1964 Declaration of Helsinki and its later amendments or comparable ethical standards.

Experimental animals with diabetic nephropathy

The experimental group consisted of C57BL/6 male mice (20–22 g, aged 7 weeks) that were purchased from Koatech (Kyeonggi-do, Korea) and acclimated to laboratory conditions for one week. A specific pathogen-free animal facility was used for raising male *Postn*-null mice (C57BL/6; 129-Postntm1Jmol/J; the Jackson Laboratory, Bar Harbor, ME, USA) at 22°C, 60–70% humidity, 5 mmH₂O air pressure, 150–300 lx illumination, and a noise level of 60 dB or less, and ventilation

was performed 10–20 times per hour.

As a DN model, this study used the unilateral nephrectomy – streptozotocin (UNXSTZ) model, which is induced by STZ administration after unilateral nephrectomy (**Figure 1**)²⁰. Unilateral nephrectomy was performed on the experimental mice. One week after UNX, the mice were injected with 50 mg/kg STZ (Sigma–Aldrich, St. Louis, MO, USA) intraperitoneally for 5 consecutive days²¹. Tail vein blood glucose levels were measured to confirm diabetes (fasting blood glucose > 300 mg/dL). The mice were sacrificed at 24 weeks post-induction of diabetes²². A spot urine sample was collected and measured for creatinine and albumin before the mice were sacrificed. The animals were randomly divided into four experimental groups: wild-type sham (WT sham), wild-type UNXSTZ (WT STZ), *Postn*-null mice sham (KO sham), and *Postn*-null mice UNXSTZ (KO STZ).

In accordance with the National Research Council’s Guidelines for the Care and Use of Laboratory Animals, the animal experiments were conducted in the animal laboratory of the Seoul National University Boramae Medical Center under pathogen-free conditions after approval from the Institutional Animal Care and Use Committee (No. 2019-0002).

Measurement of kidney function by UACR

A spot urine sample was obtained before sacrificing mice that had been maintained in the diabetic model for 24 weeks. A minimum of 100 mL of spot urine was collected. By checking the UACR level, it was confirmed that diabetic nephropathy had occurred²². Spot urine was used to measure albumin and creatinine using Albuwell M (Ethos Bioscience) and The Creatinine Companion (Ethos Bioscience)²³.

Assessment of kidney function based on creatinine levels

Whole blood was collected from the mice as well as analyzed the whole blood samples immediately on the spot using a portable clinical analyzer, i-STAT Portable Clinical Analyzer (Abbott Laboratories, Abbott Park, IL, USA), at the same time. A minimum of 100 μ l of blood was collected per mouse, and 100 μ l of whole blood was loaded into the i-STAT. i-STAT was used to determine the creatinine level in the whole blood.

Ultrasound Examination

Ultrasound exam was performed by using a commercial US scanner (Aplio i800; Canon Medical Systems) with an ultra-high-resolution linear probe (i33LX9, center frequency 33 MHz) and high-resolution linear probe (i18LX5, center frequency 18 MHz), by a board-certificated radiologist (M.S.L with 11 years of genitourinary imaging). After anesthetizing the mouse, the hair around the left flank of the mouse was shaved in a prone position, and sterilized ultrasound gel was applied. The location, size and color doppler imaging of targeted kidney was performed by using i33LX9 probe, including measurement of resistive index (RI). The RI was determined the mean value of two separated measurement from different interlobar arteries of targeted kidney. Shear-wave elastography (SWE) was performed by using i18LX5 under the display setting of 90 kPa. After sufficiently applying gel to the skin of the part to be observed, the probe was closely attached and slowly lifted vertically. When the skin was slightly pulled due to viscosity and the thickness of the ultrasonic gel was around 0.5 cm on imaging, the probe was fixed using a clamp. SWE was performed using one-shot mode, which means that the main pulse over

one frame to measure the resultant speed of the shear wave and elasticity in the tissue being examined. As seen on Figure, two or three of 1-mm diameter linear Region of Interest (ROI) was located based on the information from propagation map (Left upper of **Figure 3d**) and variation (confidence) map (Left lower image of **Figure 3d**). As the recommendation of vender, the radiologist placed the ROI in where the contour lines were most parallel and dense on the propagation map, with the lowest variation on the confidence map, and closest to the lower polar cortex on the greyscale map. After four separated shots of main pulse, 10 to 12 ROIs from four measurement were obtained. Each ROI presents the mean shear wave speed (m/s) in the ROI, as well as mean stiffness value (kPa) of the ROI calculated from the equation $E = 3\rho V_s^2$, where E is elasticity, ρ is density of the tissue, and V_s is estimated shear wave speed²⁴. The ρ value is regarded as 1 kg/m³ as the dominant component of animal body is water. The median value of speed (m/s) or stiffness (kPa) was presented as a representative value according to the guideline proposed by European Federation of Societies for Ultrasound in Medicine (EFSUMB)²⁵.

Histological analyses

Paraffin-embedded kidney tissue sections (4- μ m thick) were stained with Sirius red (all from ScyTek, Logan, Utah, USA) to evaluate the extent of tissue fibrosis. For each kidney section, at least eight fields (at a magnification of $\times 200$) were randomly selected and photographed using a light microscope (BX53F2; Olympus, Tokyo, Japan). The area of fibrosis and total tissue were measured using ImageJ 1.52d software (Wayne Rasband, National Institute of Health, USA). A minimum of 10 glomeruli per mouse kidney were evaluated at $\times 400$ magnification. The degree of Sirius red staining of the tubule and glomeruli, as well as the size of the glomeruli,

was measured using ImageJ 1.52d software (Wayne Rasband, National Institute of Health, USA) ²⁶.

Paraffin-embedded pancreatic tissue sections (4- μ m thick) were stained with periodic acid Schiff's (PAS; ScyTek, Logan, Utah, USA) to evaluate morphologic changes. A minimum of 5 pancreatic islets per mouse were selected and evaluated at $\times 200$ magnification using ImageJ 1.52d software (Wayne Rasband, National Institute of Health, USA).

Immunohistochemistry

Paraffinized kidney and pancreas tissue blocks were sliced into 4- μ m-thick sections, deparaffinized in xylene, and rehydrated in ethanol. The sliced specimens were heated in a microwave oven for 5 minutes three times with 10% citrate buffer solution (pH 6.0) to retrieve the antigen. Hydrogen peroxide (3%) in methanol was used to block endogenous streptavidin activity for 10 minutes at room temperature. Sections of the kidney were incubated overnight at 4°C with primary antibodies against POSTN and TNC. Primary antibodies against insulin and glucagon were incubated overnight at 4°C with pancreas sections. To detect rabbit and mouse primary antibodies, a Polkin HRP DAB detection kit (GBI Labs, Bothell, WA, USA) was utilized. The sections were counterstained with Mayer's hematoxylin (ScyTek Laboratories, Logan, UT, USA). The stained slides of kidney tissue were captured in at least eight selected fields and evaluated at $\times 200$ magnification. A minimum of 10 glomeruli per mouse kidney were evaluated at $\times 400$ magnification. The percentage of POSTN- and TNC-positive areas was measured by using ImageJ 1.52d software (Wayne Rasband, National Institute of Health, USA). At least five pancreatic islets were captured and evaluated at $\times 200$ magnification in the stained slide of the

pancreas. The percentages of insulin- and glucagon-positive areas of the pancreatic islets were measured by using ImageJ 1.52d software (Wayne Rasband, National Institute of Health, USA.)²⁷.

Establishment of the in vitro model

A cell model of fibroblast-myofibroblast transdifferentiation was established using NRK-49F cells, a type of renal interstitial fibroblast^{28 29}. During cultivation, the cells were maintained at 37°C, 95% air, and 5% CO₂. To prepare complete media for cell culture, 10% fetal bovine serum (FBS; Biowest, Nuaille, France) was added to Dulbecco's modified Eagle's medium (Gibco Laboratories, Grand Island, NY, USA). Following one day of starvation, in accordance with the experimental group, the cells were treated with 2 ng/ml TGF- β (R&D Systems, Wiesbaden, Germany) or 0.1 μ g/ml, 0.5 μ g/ml, or 1 μ g/ml rPOSTN (R&D Systems, Wiesbaden, Germany).

The INS-1 rat insulinoma cell line was also used in this study. Growing conditions included 37°C, 95% air, and 5% carbon dioxide. To prepare complete media for cell culture, 10% FBS (Sigma-Aldrich, St. Louis, MO, USA), 2 mM L-glutamine (Sigma-Aldrich, St. Louis, MO, USA), 1 mM sodium pyruvate (Sigma-Aldrich, St. Louis, MO, USA), 10 mM HEPES (Sigma-Aldrich, St. Louis, MO, USA), and 0.05 mM 2-mercaptoethanol (Sigma-Aldrich, St. Louis, MO, USA) were added to Dulbecco's modified Eagle's medium (Sigma-Aldrich, St. Louis, MO, USA)³⁰. INS-1 cells were treated with STZ (Sigma-Aldrich, St. Louis, MO, USA) at two concentrations, namely, 2 mM and 4 mM, and anti-POSTN antibodies were added at 0.1 μ g/ml, 0.3 μ g/ml, and 0.5 μ g/ml at each STZ concentration^{31 32}. Isotype IgG (Abcam, Cambridge, MA, USA) was treated at 0.5 μ g/ml as an anti-POSTN antibody-treated control (R&D Systems, Wiesbaden, Germany). The viability of the

cells was measured using EZ-Cytox (DoGenBio, Seoul, Korea) following the above experiment^{33 30}.

Western blot analysis

A diabetic mouse model was maintained for 24 weeks, and the kidneys and pancreas were collected at the end of the experiment. Tissues from mouse and rat kidney fibroblasts (NRK-49F) incubated for 72 hours were homogenized. The proteins were isolated from tissues and cells using RIPA buffer (Thermo Fisher, Rockford, IL, USA.). Protein concentrations in each sample were determined by the BCA assay (Thermo Scientific, Rockford, IL, USA), and western blotting was conducted using the same protein concentrations. Using sodium dodecyl sulfate/polyacrylamide gel electrophoresis (SDS/PAGE), the same amount of sample was separated based on protein size. To probe target proteins, separated proteins were transferred and immobilized onto membranes (Millipore Corporation, Bedford, MA, USA). Following the blocking of the nonspecific proteins, the membranes were incubated with specific primary antibodies overnight at 4°C. Anti-rabbit IgG or anti-mouse IgG antibodies (all from Cell Signaling Technology, Danvers, MA, USA) were used as secondary antibodies. On a chemiluminescence system (Advansta, CA, USA), protein bands were visualized and quantified using ImageJ 1.52d software (Wayne Rasband, National Institute of Health, USA).

Statistical analysis

An analysis of the data presented in this manuscript is expressed as means with standard deviations. In bar graphs, mean values are presented along with standard

deviations. The statistical analysis was conducted using IBM SPSS 20.0 and GraphPad Prism 8.0 (Graph-Pad Software, San Diego, CA). DN patients were analyzed using independent t tests to evaluate differences between groups. Mann–Whitney test and independent t test were used to compare between groups including WT STZ vs. KO STZ groups. One-way ANOVA test were applied to analysis cell culture related experiment results. $P < 0.05$ was considered statistically significant threshold.

Results

Association between kidney function and urinary POSTN and TNC levels in patients with DN

Measurement of POSTN and TNC concentrations in the urine of 200 DN patients was performed using ELISA. This study classified patients into a DN group according to the UPCR and eGFR. First, the patients were divided into four groups: UPCR<0.15 g/g; mild proteinuria (0.15≤UPCR<0.5 g/g); moderate proteinuria (0.5≤UPCR<3.5 g/g); and massive proteinuria (UPCR≥3.5 g/g). Based on the UPCR level, the POSTN concentration in urine increased proportionally ($p < 0.0001$) (**Figure 2a**). Next, the patients were divided into five groups according to the CKD stage, and the POSTN concentration increased with an increase in the CKD stage ($p = 0.0012$) (**Figure 2b**). The TNC concentration increased as the patient's CKD stage increased ($p < 0.0001$) (**Figure 2c**). The TNC concentration increased as the POSTN concentration increased ($p < 0.0001$) (**Figure 2d**).

Effect of POSTN Deficiency on reducing proteinuria and elasticity in the DN Animal Model

In the WT mice, the body weight of the sham group gradually increased for 24 weeks; however, the body weight of UNXSTZ did not increase (**Figure 3a**). At 24 weeks, the difference in body weight was significant between the two groups. On the other hand, in POSTN KO mice, body weight in both the sham and UNXSTZ groups did not increase; therefore, no significant difference was seen between the two groups. Creatinine levels were not different among the groups (**Figure 3b**). The

albumin-to-creatinine ratio in urine was also elevated in WT STZ mice, whereas for the KO STZ group, there was no significant difference between them and KO sham mice (**Figure 3c**).

The measurement of Shear-wave Elastography (SWE) of sham kidney (**Figure 3d**) and KO STZ kidney (**Figure 3e**). In each capture, the right upper image is a stiffness map (kPa), left upper image is a propagation map which shows the propagation of shear wave using contour lines, left lower image is a variation (confidence) map which represent low variation (high confidence) of stiffness value as a blue color, and right lower image is greyscale two-dimensional ultrasound image. According to elastography measurements of intrarenal elasticity, the WT STZ group demonstrated statistically significant increases in elasticity, in contrast to the KO STZ group. Comparing the KO STZ group with the WT sham and KO sham, it showed a slight increase in elasticity, but similar elasticity was observed (**Figure 3f**).

Anti-fibrotic effect of POSTN deficiency in the DN animal model

Sirius red staining revealed that a significant amount of fibrosis had developed in the WT STZ group compared to the KO STZ group (**Figure 4a**). POSTN immunohistochemistry (IHC) showed that the expression level of POSTN was also significantly higher in the WT STZ group, as expected (**Figure 4b**). Several measures were taken to assess the degree of fibrosis within the glomerulus. The Sirius red staining results confirmed that the degree of fibrosis progression in the glomerulus of the WT STZ group was higher than that of the other groups. By examining the degree of intraglomerular TNC staining with IHC, it was determined that the WT STZ group possessed significantly higher levels of intraglomerular TNC

accumulation than the other groups. Based on the IHC evaluation of the staining degree of POSTN in the glomeruli, the WT STZ group displayed the strongest staining degree (**Figure 4c**). According to the western blot results, Fibronectin, COL1A1, and α -SMA, a representative fibrosis marker, were increased in the WT STZ group compared to the WT sham group. The expression level of TNC, which is thought to be related to POSTN, was also higher in the WT STZ group (**Figure 4d**).

Effect of POSTN deficiency on the TGF- β 1/Smad pathway in a mouse model of kidney fibrosis

In contrast to the other groups, the WT STZ group showed significant increases in the expression levels of signaling proteins related to the TGF- β pathway. According to the study, the expression level of TGF- β increased, resulting in the upregulation of subproteins. Moreover, in the KO STZ group, the expression level of TGF- β was similar to that of the sham group, and the expression level of the subproteins was also maintained at a similar level. This study found that the quantitative differences in these TGF- β -related signals explained the differences in fibrosis severity by group (**Figure 5**).

Effect of POSTN on DN in the in vitro model

To investigate whether rPOSTN exacerbated TGF- β -induced fibrosis, TGF- β and rPOSTN were treated simultaneously. Following the observation of the morphological change, it was confirmed that the cell shape altered as a result of TGF- β treatment. In spite of the fact that rPOSTN was treated with TGF- β at the same time, cell morphology was similar to that of TGF- β alone (**Figure 6a**). Fibrosis was not

observed with rPOSTN treatment alone. According to Western analysis of the expression levels of α -SMA, COL1A1 and TNC, the degree of fibrosis was not significantly different between groups treated with TGF- β alone and TGF- β and POSTN simultaneously (**Figure 6b**).

Improving pancreatic β -cell dysfunction by POSTN deficiency

The blood glucose concentration increased in WT STZ 2 weeks after STZ injection, whereas it remained within the normal range in KO STZ. The difference in blood glucose levels between the two groups 2 weeks after STZ injections was significant. (**Figure 7a**). For the blood insulin concentration, the WT STZ group had a significantly lower insulin concentration than the other groups, while the KO STZ group maintained a high blood insulin concentration, indicating the reason for the difference in blood insulin concentration (**Figure 7b**).

When the size of islets in the pancreas was compared between the WT STZ group and the other groups, it was found that the size of the islets was significantly reduced in the WT STZ group. The KO STZ group, however, showed islet sizes similar to those observed in the KO sham group. Furthermore, it was evident that the integrity of the islet had been preserved in the KO STZ; however, this was not the case in the WT STZ group. In addition, when the insulin expression level in the islets was compared, the expression level of insulin sharply decreased in the WT STZ group, while the expression level of insulin in the KO STZ group was similar to that of the KO sham group. A high level of glucagon expression was also observed in the WT STZ group, while in the KO STZ group, it was maintained at a level similar to that of the KO sham group (**Figure 7c**). Compared to the other groups, the WT STZ group showed the highest expression levels of TNC and POSTN in the pancreas,

while the KO STZ group demonstrated similar expression levels to the sham group. In the WT STZ group, the level of glucagon expression was the highest, and in the KO STZ group, it was similar to the level of expression in the sham group (**Figure 7d**).

The apoptosis rate increased in proportion to the STZ concentration when STZ was administered to insulin-producing INS-1 cells. In the STZ-treated state, INS-1 cells became more viable as more anti-POSTN IgG treatment was applied. INS-1 cells treated with isotype IgG in addition to STZ had no statistically significant difference in viability from cells treated with STZ alone. As a result of anti-POSTN IgG treatment, cell viability increased, but it was not just an antibody effect (**Figure 7e**).

Discussion

The purpose of this study was to examine the prognostic significance of POSTN levels in patients with DN. There was a significant association between high POSTN levels and poor kidney function. The role of POSTN in DN was also examined through UNXSTZ (*in vivo* model) and experiments using NRK-49F and INS-1 cells (*in vitro* models). As a result of the experiment, it was possible to prevent kidney fibrosis and lower blood sugar levels in individuals with disease by blocking POSTN. In this study, the patients were divided into four groups on the basis of their UPCR values: UPCR<0.15 g/g; mild proteinuria ($0.15 \leq \text{UPCR} < 0.5$ g/g); moderate proteinuria ($0.5 \leq \text{UPCR} < 3.5$ g/g); and massive proteinuria ($\text{UPCR} \geq 3.5$ g/g) ³⁴. Additionally, the same patients as above were divided into five groups according to CKD stage. This study found that the urine POSTN concentration increased as the UPCR level and stage of CKD increased in the DN patient group. According to the results of the above experiments, urinary POSTN concentration increased with the deterioration of renal function in patients with DN. These findings were similar to previous study, which was conducted in nondiabetic CKD and IgA nephropathy ¹³. In CKD, POSTN plays an important role in the development of kidney fibrosis ¹⁸. These results are in agreement with the present study. To determine the different roles of POSTN in kidney fibrosis in DN from nondiabetic CKD, this study was conducted.

As a matricellular protein (MCP), TNC was reported to play a role as a biomarker for diabetes ³⁵. It is also known as a factor that plays an important role in the progression of CKD, similar to POSTN ^{36 37}. Furthermore, it is known that TNC and POSTN exchange positive feedback with each other to regulate each other's expression levels ³⁸. It has been shown that TNC concentrations are associated with

kidney impairment in patients with DN. In mouse kidneys with DN, as well as in the pancreas, there is a quantitative correlation between TNC and POSTN. In future studies, it will be important to go beyond the quantitative correlation between the two substances to unveil the correlation of specific molecular mechanisms of each substance in the kidneys and pancreas.

According to my results, DN-induced fibrosis was less common in the KO STZ groups than in the WT STZ groups. Fibrosis associated with DN can be explained using the TGF- β pathway³⁹. This study found a difference in the expression level of TGF- β -related signals according to the presence or absence of POSTN. Previous studies have shown that POSTN and TGF- β are closely related to CKD, which means that when TGF- β increases the expression of POSTN, the increased POSTN induces inflammatory cytokines, and consequently, TGF- β levels increase¹⁸. Thus, POSTN and TGF- β are interconnected in a vicious cycle. In CKD caused by DM, the TGF- β -related mechanism may play a major role similar to nondiabetic CKD.

Prior studies have demonstrated that POSTN induces fibrosis in tubular epithelial cells, and this has been attributed as a direct cause of kidney fibrosis¹⁸. EMT accounts for only 5% of the causes of kidney fibrosis. Induction of kidney fibrosis is predominantly caused by fibroblasts, NRK-49F cells, which are fibroblasts, were used in this study⁴⁰. Unlike tubular epithelial cells, POSTN did not play a significant role in the induction of fibrosis in fibroblasts, suggesting a different content from previous studies. There is a high probability that the absence of POSTN did not directly affect kidney fibrosis, but rather suppressed kidney fibrosis through the control of blood glucose levels. Because hyperglycemia primarily leads to glomerulosclerosis and tubular fibrosis in DN patients, the aforementioned hypothesis is supported⁴¹.

In the present study, it was also found that *Postn*-null mice did not have hyperglycemia because they exhibited preserved insulin secretory function even after STZ injections compared with WT mice. Additionally, when INS-1 cells and pancreatic islet β -cells were treated with a neutralizing POSTN antibody under STZ-treated conditions, their viability was improved. According to the results of the experiment, POSTN results in a reduction in the secretion of insulin. To my knowledge, my work is the first to demonstrate that POSTN directly plays a role in the deterioration of pancreatic functions, although the exact mechanism by which POSTN affects pancreatic cell viability remains unidentified at the molecular level.

One previous study showed contradictory results wherein *Postn*-null mice exhibited impaired mesenchymal formation of the pancreas and reduced regeneration after partial pancreatectomy⁴². In that study, the *Postn*-null mouse group also showed increased blood glucose, decreased insulin secretion, and fewer beta cells than the WT mice⁴². Another study also showed that *Postn*-null mice in the acute pancreatitis model did not recover their exocrine pancreatic function well⁴³. POSTN plays a crucial role in exocrine regeneration after severe acute pancreatitis⁴³. Both papers examined the role of POSTN in pancreatic structure and function, and their results contradict my findings. Although the reason for the increased level of glucagon in the WT STZ group has yet to be identified, it remains unknown what might be responsible for it. Further research is necessary to clarify whether POSTN directly affects alpha cells and increases their concentration of glucagon, whether it is a compensatory process due to the decrease in insulin, or whether it is related to both mechanisms.

Collectively, POSTN may have a significant effect on controlling glycemic levels in patients with type 1 diabetes, as well as preventing kidney damage caused by

POSTN. It is also possible to make more progress on this front if more research is conducted on the potential therapeutic uses of POSTN blockers in treating DN patients.

Figures

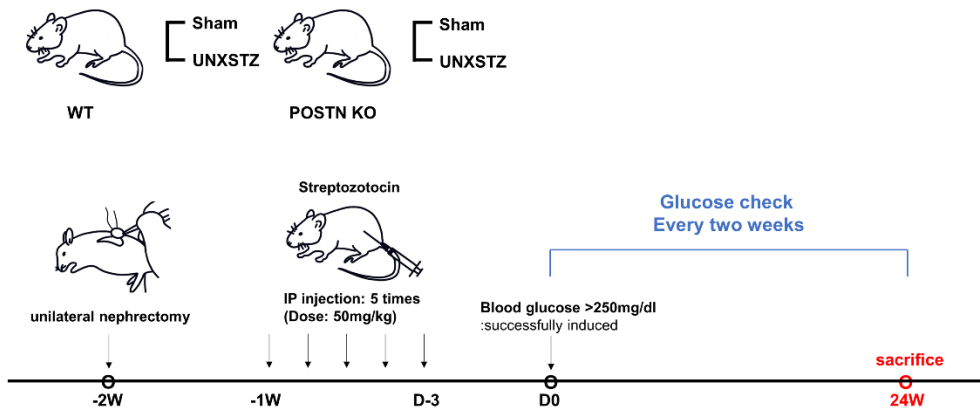


Figure 1. A schematic overview of the animal model. The diabetic nephropathy *in vivo* model was induced by streptozotocin (STZ) administration after unilateral nephrectomy (UNX). One week after UNX, the mice were injected with 50 mg/kg STZ intraperitoneally for 5 consecutive days. Tail vein blood glucose levels were measured to confirm diabetes (fasting blood glucose > 300 mg/dL). The mice were sacrificed at 24 weeks post-induction of diabetes.

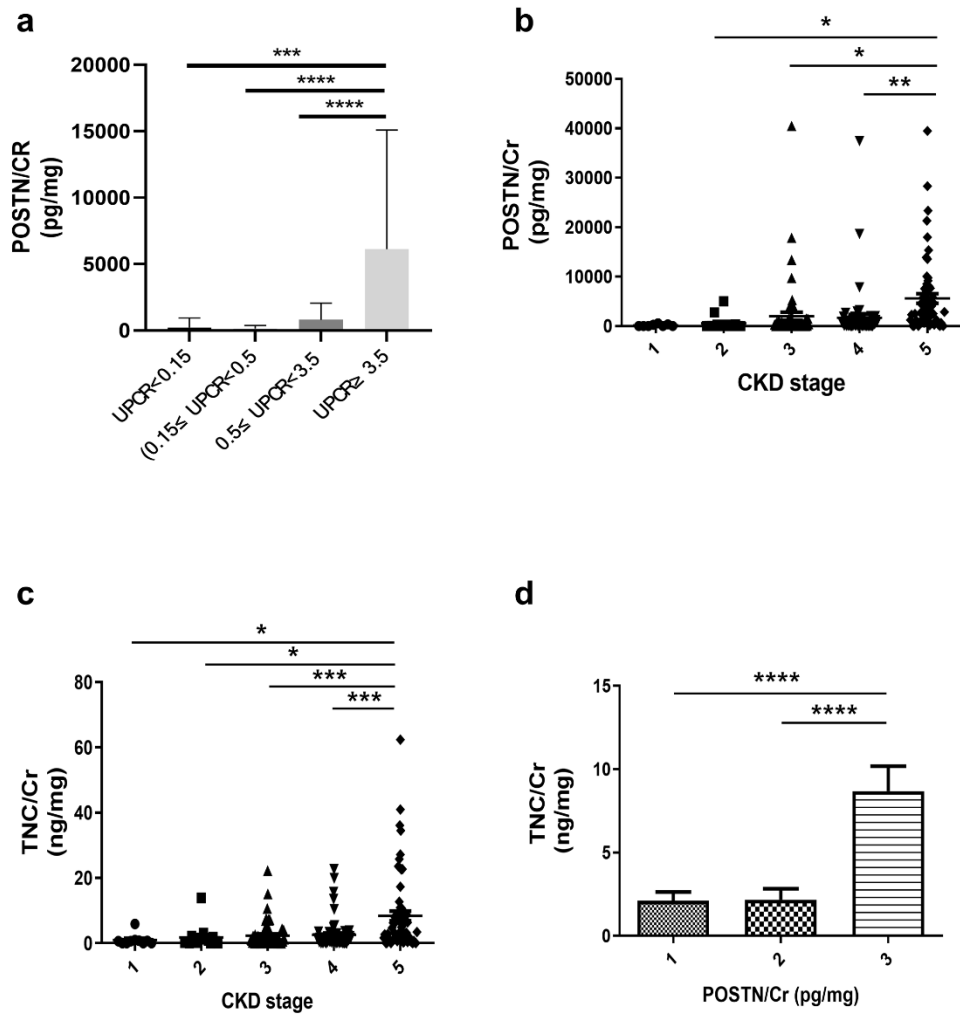


Figure 2. Periostin and tenascin C levels measured in urine in patients with diabetic nephropathy. (a) The concentration of POSTN in urine based on the UPCR value (N =207). (b) POSTN urine concentration by CKD stage in DN patients (N =199). Data are the mean \pm SD. * p <0.05, *** p <0.001 (one-way ANOVA). (c) TNC urine concentration by CKD stage in DN patients (N = 207). Data are the mean \pm SD. * p <0.05, *** p <0.001 (one-way ANOVA). (d) TNC concentration changes according to the amount of POSTN in urine collected from patients with DN (N = 179). Data are the mean \pm SD. *** p <0.001 (one-way ANOVA).

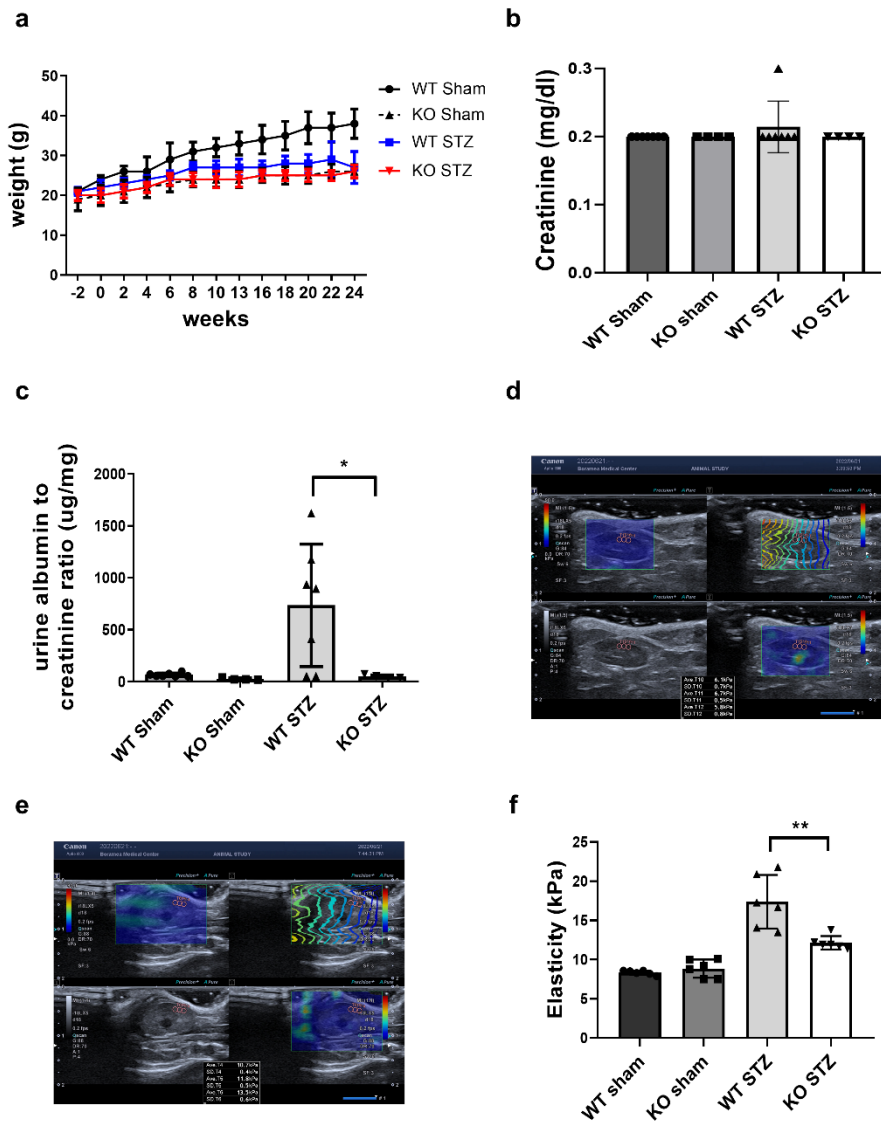
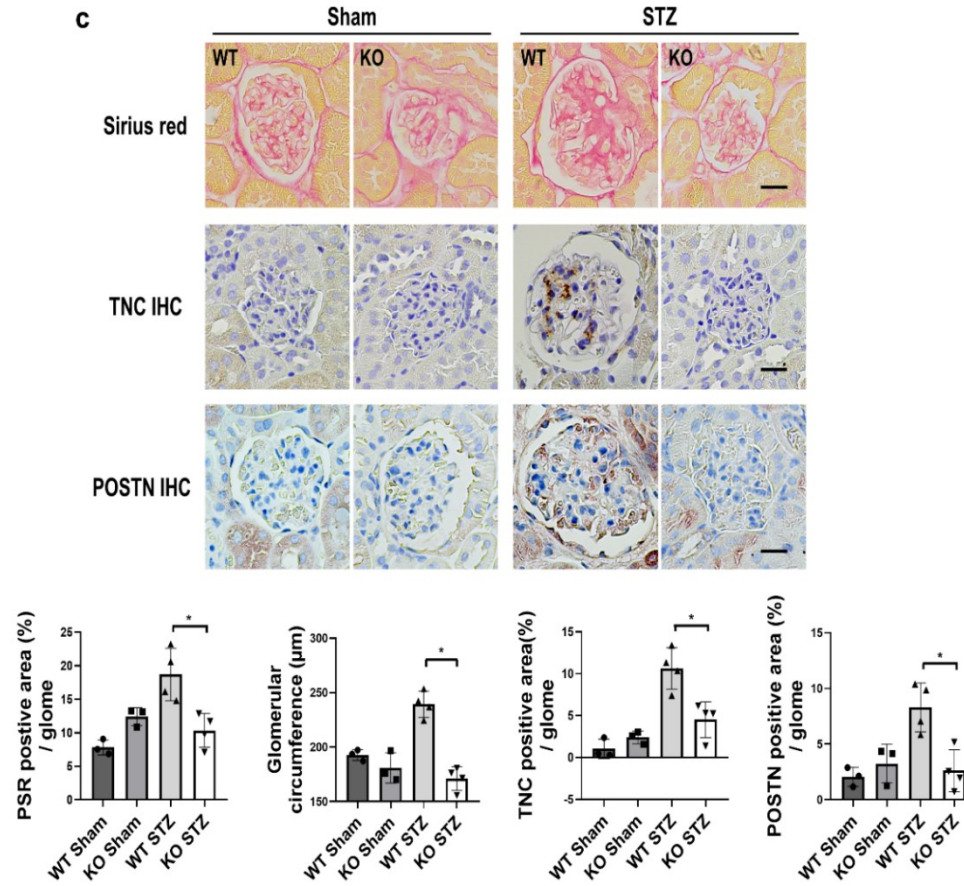
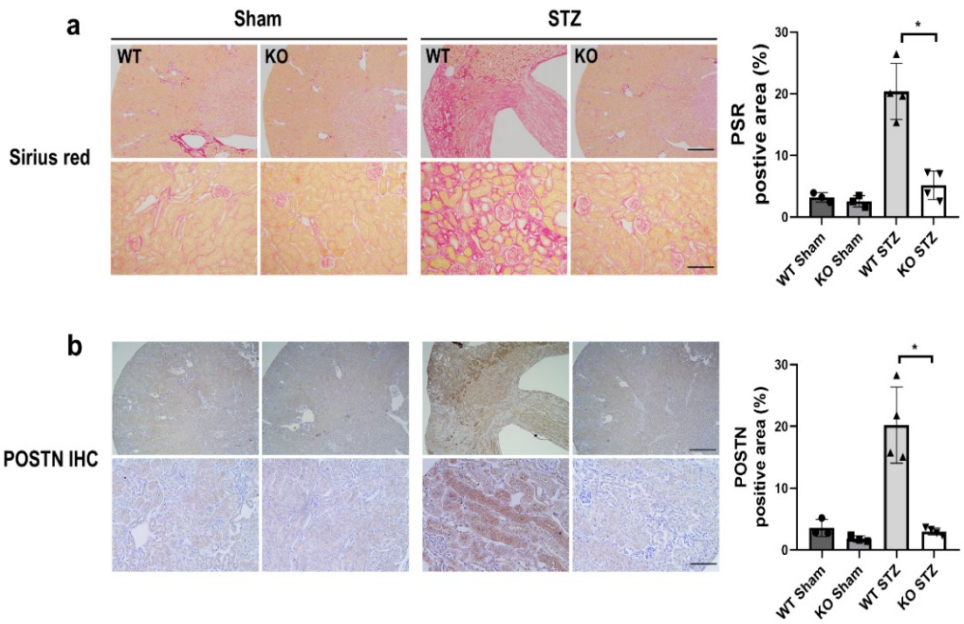


Figure 3. Functional data of the mouse groups. (a) A graph of weight changes by group for 24 weeks (WT sham, WT STZ: N = 7/group; KO sham, KO STZ: N = 4/group). (b) A comparison of creatinine measurements among groups of mice. (c) Comparative graph of the albumin/creatinine ratios among groups (WT sham, WT STZ: N = 7/group; KO sham, KO STZ: N = 4/group). Data are the mean \pm SD. * $p < 0.05$ (Mann–Whitney test). (d) The measurement of Shear-wave Elastography

(SWE) of WT sham kidney. (e) The measurement of Shear-wave Elastography (SWE) of KO STZ kidney. (f) A graph of elasticity (kPa) by group based on elastography (N = 3/group). Data are the mean \pm SD. ** $p < 0.01$ (Mann–Whitney test).



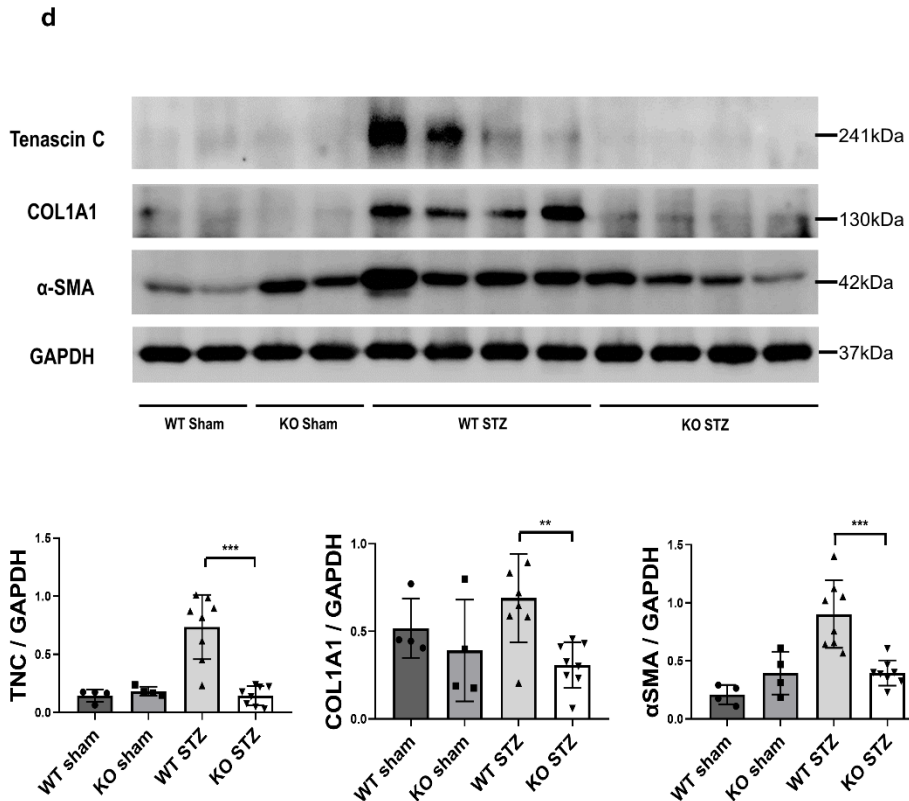


Figure 4. Analysis of data related to fibrosis among the groups of mice. (a) The degree of fibrosis progression was compared between groups based on Sirius red staining (WT sham, KO sham: N = 3/group; WT STZ, KO STZ: N = 4/group). Data are the mean \pm SD. * $p < 0.05$ (Mann–Whitney test). (b) Results of POSTN IHC staining by group (WT sham, KO sham: N = 3/group; WT STZ, KO STZ: N = 4/group). Data are the mean \pm SD. * $p < 0.05$ (Mann–Whitney test). Bar = 500 μ m. (c) The degree of intraglomerular fibrosis progression between groups was investigated using Sirius red staining and IHC staining. The glomerular circumference of each group was measured and analyzed. (WT sham, KO sham: N = 3/group; WT STZ, KO STZ: N = 4/group). Data are the mean \pm SD. * $p < 0.05$ (Mann–Whitney test). Bar = 100 μ m. (d) A comparison of fibrosis marker expression levels by group as assessed

by western blotting (WT sham, KO sham: N = 4/group; WT STZ, KO STZ: N = 8/group). Data are the mean \pm SD. ** $p < 0.01$, *** $p < 0.001$ (Mann–Whitney test).

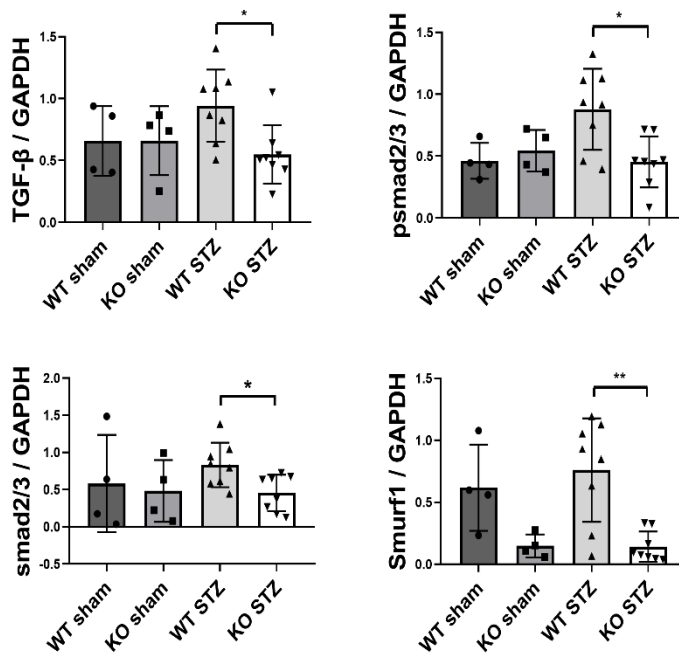
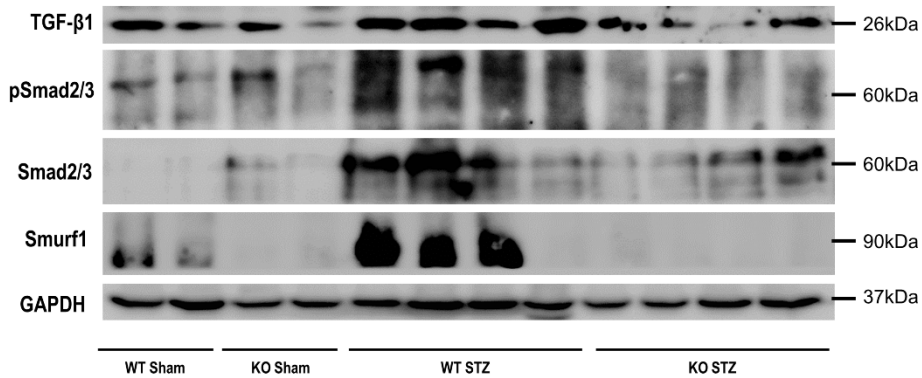


Figure 5. The effect of periostin deficiency on the TGF-β1/Smad pathway in a diabetic nephropathy model. The expression levels of TGF-β signal-related markers differed among the study groups, as shown by western blot results (WT sham, KO sham: N = 4/group; WT STZ, KO STZ: N = 8/group). Data are the mean ± SD. *p<0.05, **p<0.01 (Mann-Whitney test).

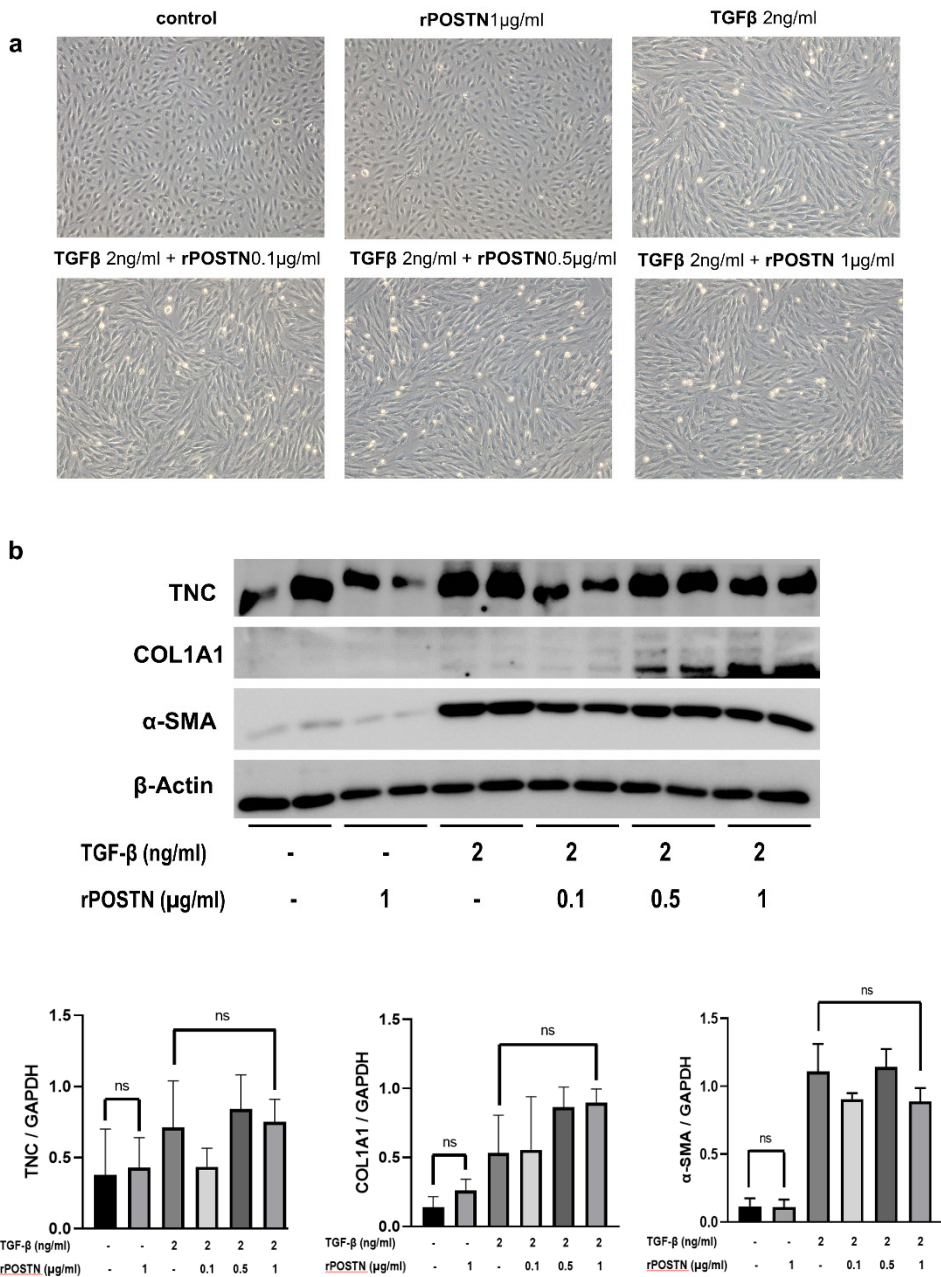
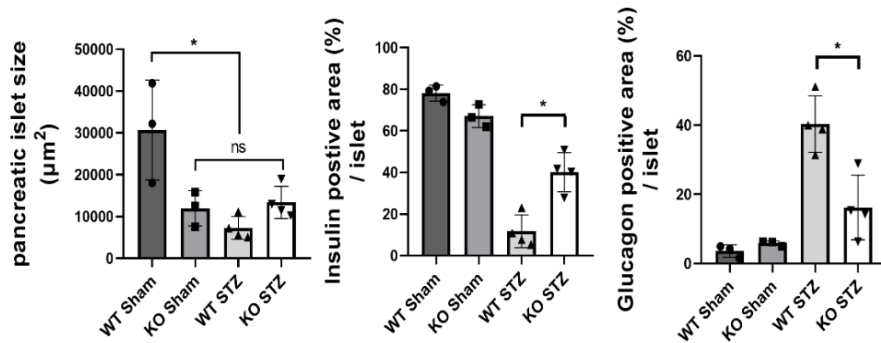
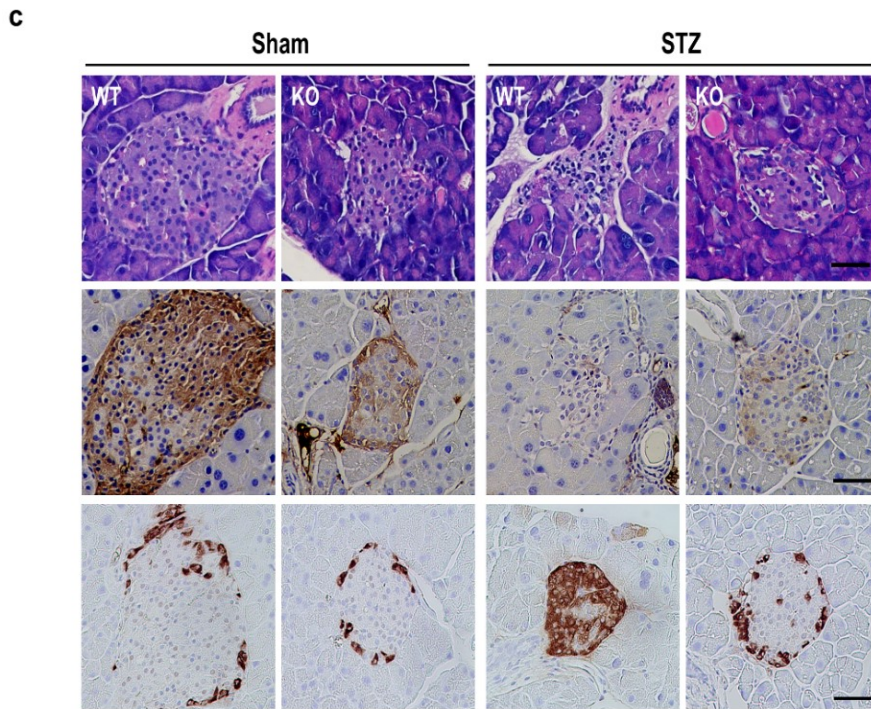
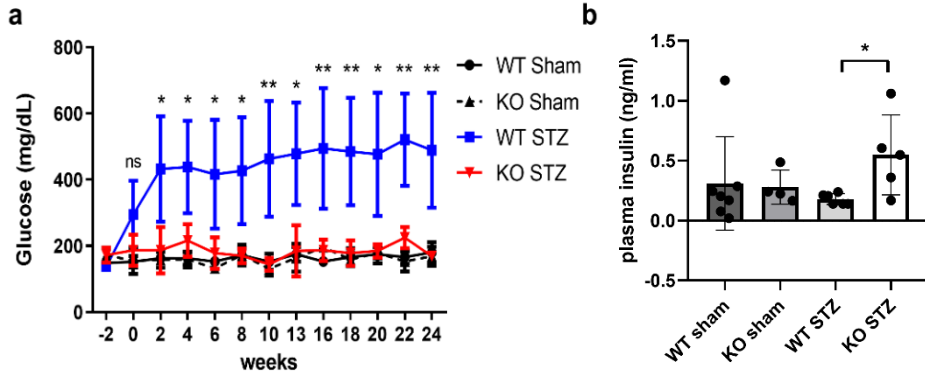
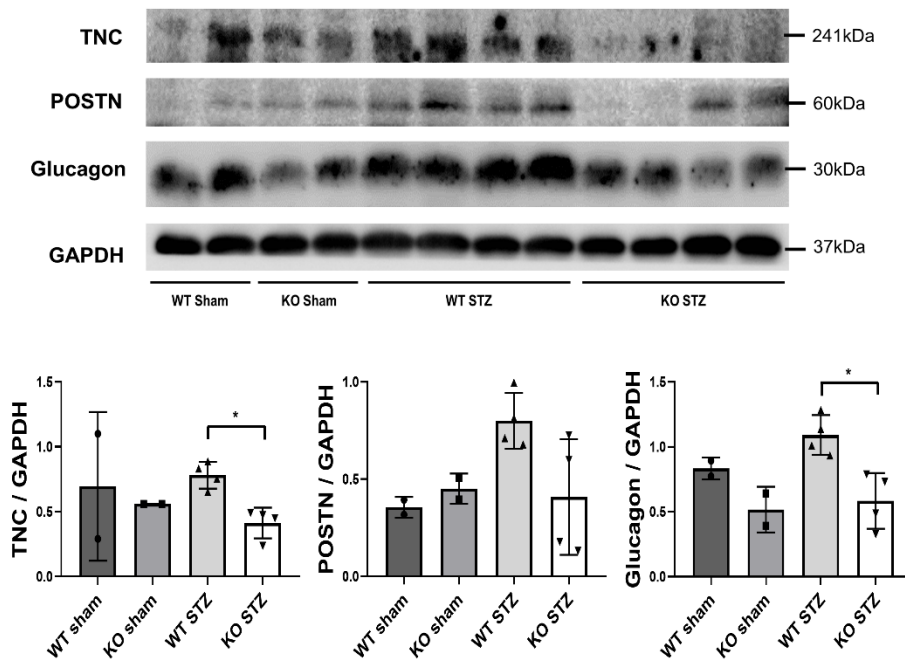


Figure 6. TGF-β and periostin-induced fibrosis in NRK-49 cells. (a) Morphological changes in NRK-49F cells after treatment with TGF-β and rPOSTN. (b) Western blot results presenting a change in the expression of TNC, COL1A1 when NRK-49F cells were treated with TGF-β and POSTN simultaneously or separately (N = 5 /group). Data are the mean ± SD. ns (one-way ANOVA test).



d



e

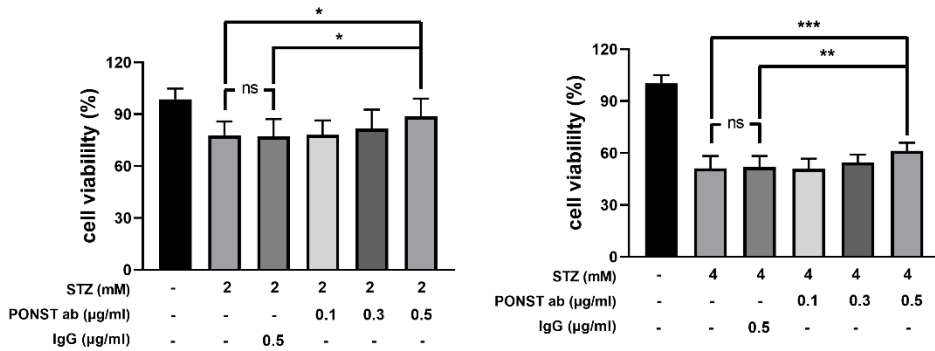


Figure 7. The role of POSTN in pancreatic function. (a) Changes in blood glucose levels by group observed during the 24-week study (WT sham, WT STZ: N = 7/group; KO sham, KO STZ: N = 4/group). Data are the mean \pm SD. * p <0.05, ** p <0.01 (Mann–Whitney test). (b) A comparison of blood insulin levels between groups (WT sham, WT STZ: N = 6/group; KO sham, KO STZ: N = 4/group). Data are the mean \pm SD. * p <0.05 (Mann–Whitney test). (c) Morphological changes

between groups of pancreatic islets as evidenced by PAS staining (WT sham, KO sham: N = 3/group; WT STZ, KO STZ: N = 4/group). The IHC staining results indicate differences between groups in insulin and glucagon expression. Data are the mean \pm SD. * p <0.05 (unpaired t test). Bar = 50 μ m. (d) A comparison of POSTN, TNC, insulin, and glucagon expression levels in pancreatic tissue by group (WT sham, KO sham: N = 2/group; WT STZ, KO STZ: N = 4/group). Data are the mean \pm SD. * p <0.05 (Mann–Whitney test). (e) An analysis of INS-1 cell viability when treated with STZ and neutralizing POSTN antibodies (N = 12/group). Data are the mean \pm SD. * p <0.05, ** p <0.01, *** p <0.001 (one-way ANOVA test).

Reference

1. Wang G, Ouyang J, Li S, Wang H, Lian B, Liu Z, et al.: The analysis of risk factors for diabetic nephropathy progression and the construction of a prognostic database for chronic kidney diseases. *Journal of Translational Medicine*, 17: 1-12, 2019
2. Morra L, Moch H: Periostin expression and epithelial-mesenchymal transition in cancer: a review and an update. *Virchows Archiv*, 459: 465-475, 2011
3. Conway SJ, Izuhara K, Kudo Y, Litvin J, Markwald R, Ouyang G, et al.: The role of periostin in tissue remodeling across health and disease. *Cellular and Molecular Life Sciences*, 71: 1279-1288, 2014
4. Jia G, Erickson RW, Choy DF, Mosesova S, Wu LC, Solberg OD, et al.: Periostin is a systemic biomarker of eosinophilic airway inflammation in asthmatic patients. *Journal of Allergy and Clinical Immunology*, 130: 647-654. e610, 2012
5. Zhao S, Wu H, Xia W, Chen X, Zhu S, Zhang S, et al.: Periostin expression is upregulated and associated with myocardial fibrosis in human failing hearts. *Journal of cardiology*, 63: 373-378, 2014
6. Ling L, Cheng Y, Ding L, Yang X: Association of serum periostin with cardiac function and short-term prognosis in acute myocardial infarction patients. *PLoS One*, 9: e88755, 2014
7. Kudo Y, Siriwardena B, Hatano H, Ogawa I, Takata T: Periostin: novel diagnostic and therapeutic target for cancer. *Histology and histopathology*, 2007
8. Ruan K, Bao S, Ouyang G: The multifaceted role of periostin in tumorigenesis. *Cellular and molecular life sciences*, 66: 2219-2230, 2009
9. Underwood TJ, Hayden AL, Derouet M, Garcia E, Noble F, White MJ, et al.: Cancer-associated fibroblasts predict poor outcome and promote periostin-dependent invasion in oesophageal adenocarcinoma. *The Journal of pathology*, 235: 466-477, 2015
10. Satirapoj B, Wang Y, Chamberlin MP, Dai T, LaPage J, Phillips L, et al.: Periostin: novel tissue and urinary biomarker of progressive renal injury induces a coordinated mesenchymal phenotype in tubular cells. *Nephrology Dialysis Transplantation*, 27: 2702-2711, 2012
11. Satirapoj B, Tassanasorn S, Charoenpitakchai M, Supasyndh O: Periostin as a tissue and urinary biomarker of renal injury in type 2 diabetes mellitus. *PLoS One*, 10: e0124055, 2015

12. Wantanasiri P, Satirapoj B, Charoenpitakchai M, Aramwit P: Periostin: a novel tissue biomarker correlates with chronicity index and renal function in lupus nephritis patients. *Lupus*, 24: 835-845, 2015
13. Hwang JH, Lee JP, Kim CT, Yang SH, Kim JH, An JN, et al.: Urinary periostin excretion predicts renal outcome in IgA nephropathy. *American Journal of Nephrology*, 44: 481-492, 2016
14. Braun N, Sen K, Alscher MD, Fritz P, Kimmel M, Morelle J, et al.: Periostin: a matricellular protein involved in peritoneal injury during peritoneal dialysis. *Peritoneal Dialysis International*, 33: 515-528, 2013
15. Sen K, Lindenmeyer MT, Gaspert A, Eichinger F, Neusser MA, Kretzler M, et al.: Periostin is induced in glomerular injury and expressed de novo in interstitial renal fibrosis. *The American journal of pathology*, 179: 1756-1767, 2011
16. Guerrot D, Dussaule J-C, Mael-Ainin M, Xu-Dubois Y-C, Rondeau E, Chatziantoniou C, et al.: Identification of periostin as a critical marker of progression/reversal of hypertensive nephropathy. *PLoS One*, 7: e31974, 2012
17. Hwang JH, Yang SH, Kim YC, Kim JH, An JN, Moon KC, et al.: Experimental inhibition of periostin attenuates kidney fibrosis. *American journal of nephrology*, 46: 501-517, 2017
18. An JN, Yang SH, Kim YC, Hwang JH, Park JY, Kim DK, et al.: Periostin induces kidney fibrosis after acute kidney injury via the p38 MAPK pathway. *American Journal of Physiology-Renal Physiology*, 316: F426-F437, 2019
19. An JN, Kim H, Kim EN, Cho A, Cho Y, Choi YW, et al.: Effects of periostin deficiency on kidney aging and lipid metabolism. *Aging (Albany NY)*, 13: 22649, 2021
20. Wada J, Zhang H, Tsuchiyama Y, Hiragushi K, Hida K, Shikata K, et al.: Gene expression profile in streptozotocin-induced diabetic mice kidneys undergoing glomerulosclerosis. *Kidney international*, 59: 1363-1373, 2001
21. Yung S, Chau MK, Zhang Q, Zhang CZ, Chan TM: Sulodexide decreases albuminuria and regulates matrix protein accumulation in C57BL/6 mice with streptozotocin-induced type I diabetic nephropathy. *PLoS One*, 8: e54501, 2013
22. Bai X, Li X, Tian J, Xu L, Wan J, Liu Y: A new model of diabetic nephropathy in C57BL/6 mice challenged with advanced oxidation protein products. *Free Radical Biology and Medicine*, 118: 71-84, 2018

23. Riera M, Márquez E, Clotet S, Gimeno J, Roca-Ho H, Lloreta J, et al.: Effect of insulin on ACE2 activity and kidney function in the non-obese diabetic mouse. *PLoS one*, 9: e84683, 2014
24. Nightingale K: Acoustic radiation force impulse (ARFI) imaging: a review. *Current medical imaging*, 7: 328-339, 2011
25. Săftoiu A, Gilja OH, Sidhu PS, Dietrich CF, Cantisani V, Amy D, et al.: The EFSUMB guidelines and recommendations for the clinical practice of elastography in non-hepatic applications: update 2018. *Ultraschall in der Medizin-European Journal of Ultrasound*, 40: 425-453, 2019
26. Uil M, Scantlebery AM, Butter LM, Larsen PW, de Boer OJ, Leemans JC, et al.: Combining streptozotocin and unilateral nephrectomy is an effective method for inducing experimental diabetic nephropathy in the 'resistant' C57Bl/6J mouse strain. *Scientific Reports*, 8: 1-10, 2018
27. Murai N, Ohtaki H, Watanabe J, Xu Z, Sasaki S, Yagura K, et al.: Intrapancreatic injection of human bone marrow-derived mesenchymal stem/stromal cells alleviates hyperglycemia and modulates the macrophage state in streptozotocin-induced type 1 diabetic mice. *PLoS One*, 12: e0186637, 2017
28. Vega G, Alarcón S, San Martín R: The cellular and signalling alterations conducted by TGF- β contributing to renal fibrosis. *Cytokine*, 88: 115-125, 2016
29. Yi Y, Ma J, Jianrao L, Wang H, Zhao Y: WISP3 prevents fibroblast–myofibroblast transdifferentiation in NRK-49F cells. *Biomedicine & Pharmacotherapy*, 99: 306-312, 2018
30. Ko EJ, Shin YJ, Cui S, Lim SW, Chung BH, Yang CW: Effect of dual inhibition of DPP4 and SGLT2 on tacrolimus-induced diabetes mellitus and nephrotoxicity in a rat model. *American Journal of Transplantation*, 2022
31. Kim J, Shin S-H, Kang J-K, Kim JW: HX-1171 attenuates pancreatic β -cell apoptosis and hyperglycemia-mediated oxidative stress via Nrf2 activation in streptozotocin-induced diabetic model. *Oncotarget*, 9: 24260, 2018
32. Lin Y, Xu Y, Zheng X, Zhang J, Liu J, Wu G: Astragaloside IV Ameliorates Streptozotocin Induced Pancreatic β -Cell Apoptosis and Dysfunction Through SIRT1/P53 and Akt/GSK3 β /Nrf2 Signaling Pathways. *Diabetes, Metabolic Syndrome and Obesity: Targets and Therapy*, 15: 131, 2022
33. Zheng S, Zhao M, Ren Y, Wu Y, Yang J: Sesamin suppresses STZ induced INS-

- 1 cell apoptosis through inhibition of NF- κ B activation and regulation of Bcl-2 family protein expression. *European journal of pharmacology*, 750: 52-58, 2015
34. Wang S, Wang F, Wang X, Zhang Y, Song L: Elevated Creatinine Clearance in Lupus Nephritis Patients with Normal Creatinine. *International Journal of Medical Sciences*, 18: 1449, 2021
35. Yonebayashi S, Tajiri K, Li S, Sato A: Tenascin-C: an emerging prognostic biomarker in diabetes. *Annals of Translational Medicine*, 8, 2020
36. Zhu H, Liao J, Zhou X, Hong X, Song D, Hou FF, et al.: Tenascin-C promotes acute kidney injury to chronic kidney disease progression by impairing tubular integrity via $\alpha\beta 6$ integrin signaling. *Kidney international*, 97: 1017-1031, 2020
37. Zou C, Xie R, Bao Y, Liu X, Sui M, Li S, et al.: Iron chelator alleviates tubulointerstitial fibrosis in diabetic nephropathy rats by inhibiting the expression of tenascinC and other correlation factors. *Endocrine*, 44: 666-674, 2013
38. Okada T, Suzuki H: The role of tenascin-C in tissue injury and repair after stroke. *Frontiers in Immunology*, 11: 607587, 2021
39. Shen Y-L, Jiang Y-p, Li X-Q, Wang S-J, Ma M-H, Zhang C-Y, et al.: ErHuang formula improves renal fibrosis in diabetic nephropathy rats by inhibiting CXCL6/JAK/STAT3 signaling pathway. *Frontiers in pharmacology*, 10: 1596, 2020
40. LeBleu VS, Taduri G, O'connell J, Teng Y, Cooke VG, Woda C, et al.: Origin and function of myofibroblasts in kidney fibrosis. *Nature medicine*, 19: 1047-1053, 2013
41. Sun H-J, Wu Z-Y, Cao L, Zhu M-Y, Liu T-T, Guo L, et al.: Hydrogen sulfide: recent progression and perspectives for the treatment of diabetic nephropathy. *Molecules*, 24: 2857, 2019
42. Smid JK, Faulkes S, Rudnicki MA: Periostin induces pancreatic regeneration. *Endocrinology*, 156: 824-836, 2015
43. Hausmann S, Regel I, Steiger K, Wagner N, Thorwirth M, Schlitter AM, et al.: Loss of periostin results in impaired regeneration and pancreatic atrophy after cerulein-induced pancreatitis. *The American journal of pathology*, 186: 24-31, 2016

국문 초록

POSTN 결여로 인한 췌장 β -세포 기능장애 개선에 따른 당뇨병 콩팥병 완화 효과

조 아 라
의학과 중개의학전공
The Graduate School
Seoul National University

서론: 만성 신장 질환의 가장 흔한 원인인 당뇨병 콩팥병(DN)은 신장 섬유증과 관련이 있다. 이전 연구에서 periostin (POSTN)이 신장 섬유증에서 중요한 역할을 한다는 것을 입증했다. 해당 연구에서는 당뇨병 콩팥병에서 POSTN의 역할을 조사하였다.

방법: 당뇨병 콩팥병 환자의 소변 샘플에서 POSTN 및 tenascin C (TNC) 농도를 측정했다. 마우스에 편측 신장 절제술(UNXSTZ)을 진행한 후 50mg/kg streptozotocin (STZ)은 5일 동안 투여하여 WT 및 *Postn*-null mice 모두에서 당뇨병 콩팥병 모델을 구축하였다. 실험군은 총 4개의 실험 그룹: wild-type sham (WT sham), wild-type UNXSTZ (WT STZ), *Postn*-null mice sham (KO sham), *Postn*-null

mice UNXSTZ (KO STZ)으로 구성되어 있다. 20주 후, 섬유화 관련 마커의 분자 발현 및 조직학적 변화를 평가하였다. 또한 실험 마우스의 혈당 수치와 소변 알부민을 주기적으로 측정하였다. 당뇨병 콩팥병의 세포 모델로서 NRK 49F 세포를 TGF- β 처리 하에 배양하였고, STZ으로 INS-1 세포를 자극한 뒤 cell viability를 측정하였다.

결과: 인체 시료에서 당뇨병 콩팥병의 중증도에 따라 POSTN 및 TNC의 농도가 증가하였다. WT STZ 모델과 비교하여 KO STZ 모델은 소변 알부민 배설이 낮고 사구체 경화증 및 간질 섬유증이 적었다. 또한 KO STZ 모델은 섬유증 마커 발현 및 TNC의 발현이 더 낮았다. KO STZ 모델의 혈당 수준은 WT STZ 모델과 비교하여 잘 조절되었을 뿐만 아니라 췌장조직의 완전성 및 인슐린 발현이 유의하게 더 많이 보존되었다. 세포 모델에서는 NRK-49F 세포를 이용하여 TGF- β 와 rPOSTN을 동시에 처리함으로써 fibrosis 진행 정도를 확인하였지만 TGF- β 단독 처리와 별다른 차이가 없었다. INS-1 세포에 STZ 처리시 항 POSTN antibody를 처리할 경우 STZ 단독 처리보다 더 높은 cell viability를 나타냈다.

결론: POSTN의 기여는 당뇨병 콩팥병에서 췌장 β 세포 기능 개선을 통한 신장 섬유 완화에서 필수적인 역할을 한다. POSTN 차단은 당뇨병 콩팥병의 새로운 치료법이 될 가능성을 보여준다.

Keyword: POSTN; 당뇨병 콩팥병; 신장 섬유화; TNC; 베타세포 기능
장애; UNXSTZ

Student Number: 2020-26768